Microstructures and Hardness of TIG Welded Experimental 57Fe15Cr25Ni Steel

Parikin Parikin
Center for Science and Technology of Advanced Materials, National Nuclear Energy Agency (BATAN), Puspiptek Area, South Tangerang 15314, Indonesia, farihin@batan.go.id

Mohammad Dani
Center for Science and Technology of Advanced Materials, National Nuclear Energy Agency (BATAN), Puspiptek Area, South Tangerang 15314, Indonesia

Abu Khalid Rivai
Center for Science and Technology of Advanced Materials, National Nuclear Energy Agency (BATAN), Puspiptek Area, South Tangerang 15314, Indonesia

Agus Hadi Ismoyo
Center for Science and Technology of Advanced Materials, National Nuclear Energy Agency (BATAN), Puspiptek Area, South Tangerang 15314, Indonesia

Riza Iskandar
Central Facility for Electron Microscopy (GFE), RWTH Aachen University, Ahorn strasse 55, D-52074 Aachen, Germany

Follow this and additional works at: https://scholarhub.ui.ac.id/mjt

Part of the Chemical Engineering Commons, Civil Engineering Commons, Computer Engineering Commons, Electrical and Electronics Commons, Metallurgy Commons, Ocean Engineering Commons, and the Structural Engineering Commons

See next page for additional authors

Recommended Citation

Microstructures and Hardness of TIG Welded Experimental 57Fe15Cr25Ni Steel

Authors

Parikin Parikin, Mohammad Dani, Abu Khalid Rivai, Agus Hadi Ismoyo, Riza Iskandar, and Arbi Dimyati

Microstructures and Hardness of TIG Welded Experimental 57Fe15Cr25Ni Steel

Parikin[1*], Mohammad Dani[1], Abu Khalid Rivai[1], Agus Hadi Ismoyo[1], Riza Iskandar[2], and Arbi Dimyati[1]

1. Center for Science and Technology of Advanced Materials, National Nuclear Energy Agency (BATAN), Puspiptek Area, South Tangerang 15314, Indonesia
2. Central Facility for Electron Microscopy (GFE), RWTH Aachen University, Ahorn strasse 55, D-52074 Aachen, Germany

*e-mail: farihin@batan.go.id

Abstract

The microstructures and hardness of tungsten inert gas (TIG) welded experimental 57Fe15Cr25Ni steel were investigated through optical–scanning electron microscopy analyses and with a hardness tester, respectively. The welding process restructured the constituent atoms into regular and irregular crystal lattices. Rapid cooling of the weld metal allowed the formation of a dendritic (columnar) structure, with porous grains. By contrast, slow cooling influenced HAZ and led to the formation of grain structures. The crystal lattice became more organized and larger than other zones. Meanwhile, the base metal formed circular nets that covered large area inside thick and thin grain boundaries. The diffraction patterns revealed texturing in the weld metal. The crystallite orientation changed from (111) to (200) and (220) planes. The weld metal profile broadened (amorphous) and had full width at half maximum (fwhm) value larger than those in HAZ and the base metal. The weld metal possessed hardness of 121 HV, which is slightly lower than the hardness of the base metal (130 HV). HAZ exhibited the highest hardness value (152 HV). Hardening was influenced by carbon and outer oxygen migration to the grain boundaries, which formed colonies, i.e., chromium carbide, aluminum carbide, aluminum oxide, silicone oxide, and silicon carbide (precipitation hardening). Welding (heat) may change the microstructure and hardness of HAZ and the weld metal region, which would be brittle and very critical in responding to applied loads.

Abstrak

Struktur Mikro dan Kekerasan pada Las TIG Baja Experimental 57Fe15Cr25Ni. Pengamatan pengaruh panas las pada pembentukan struktur mikro dan kekerasan plat baja 57Fe15Cr25Ni menggunakan mikroskop optik (*OM*) - electron (*SEM*), dan *Microhardness Vickers Testing Machine* yang berindenter *diamond* telah dilakukan. Hasil memperlihatkan bahwa mekanisme panas las mampu mempengaruhi proses penataan ulang atom-atom penyusun kisi kristal menjadi teratur dan tidak teratur. Karena mengalami pendinginan yang cepat, struktur mikro pusat las (*weld metal*) berbentuk dendrit columnar berpori dalam lingkupan struktur matriks, sedang efek pendinginan melambat di daerah HAZ mengakibatkan penyusunan kisi kristal menjadi lebih teratur dan berukuran lebih besar daripada ukuran butir matrik. Di daerah logam matrik (*base metal*) struktur mikro berbentuk jejaring melingkar besar dan kecil yang dilingkupi batas butir (*grain boundary*) tebal dan tipis. Texturing terdeteksi di daerah pusat las. Kristal mengubah orientasi dari bidang refleksi (111) ke bidang refleksi (200) dan (220). Profil pusat las melebar (amorf), menyebabkan angka lebar setengah puncak maksimum (fwhm) lebih besar dari pada daerah HAZ dan basemetal, dan sangat sesuai dengan pengamatan struktur mikro permukaan bahan. Nilai rerata kekerasan pada daerah *weld metal* sekitar 121 HV, lebih rendah daripada daerah *base metal* sekitar 130 HV, sedang daerah HAZ memiliki nilai rerata kekerasan yang paling tinggi sekitar 152 HV. Pengerasan ini juga dipengaruhi oleh migrasi carbon dan oxygen luar ke batas butir (*precipitation hardening*) dan membentuk koloni seperti: chrom carbide, aluminum carbide, aluminum oxide, silicone oxide and silicon carbide. Disimpulkan bahwa panas las dapat mempengaruhi pembentukan struktur mikro dan sifat mekanik (kekerasan) bahan di daerah HAZ dan inti lasan. Kedua daerah ini dapat menjadi rapuh (*brittle*) dan sangat kritis dalam merespon beban terpakai.

Keywords: 57Fe15Cr25Ni steel, hardness, microstructure, crystal structure, TIG weld

1. Introduction

Research materials in BATAN should satisfy the general requirements of reactor structural materials in terms of tolerance to mechanical loads, high temperature and pressure, corrosion, and irradiation. These requirements are important for development of structural materials for nuclear reactors construction; according to the policy of the Research and Development department of the Center for Science and Technology of Advanced Materials (PSTBM) for reactor structural materials, BATAN engineers should have developed a series of austenitic and ferritic steel independently [1]. Research on steel series is important for application to high-temperature reactor operation.

Experimental austenitic steel synthesized through casting [2] in Bandung is a low-carbon product. This material exhibits superior properties [3] in terms of corrosion resistance in demin water (0.088 mpy), hardness (160 HVN), impact strength (1.3 J/mm^2), and tensile strength (290 MPa). The texture of this type of steel is strongly influenced by the direction of the crystal orientation of the material [4]. Moreover, tensile stress is the residual stress due to hot rolling [5], which enhances strain hardening, leading to residual stress distribution in the material.

Welding capability/weldability is one of the required properties of engineering materials [6,7]. This property is important for assessment of the reliability of engineering materials at an extremely high temperature such as in welding. The four areas formed during welding are weld center (weld metal), heat affected zone (HAZ), thermo-mechanically affected zone (TMAZ), and base metal (BM). In 2015, a study investigated the effects of welding on austenitic steel plate containing 57%Fe15%Cr25%Ni [8]. This work hypothesized that the most critical steel structure occurred in metal connections (weld joints) where the concentrations of stress and residual stress are very high. Welding also initiates the origins of cracks caused by the momentary extreme temperature (~1000 °C) [9]. In material applications, cracks can easily, suddenly (brittle fracture), or slowly (fatigue, creep, or corrosion) grow. The different types of cracks and their respective causes must be studied. Different weld treatments are usually performed to eliminate crack variation. For example, reheat cracks are removed by low-heat input welding, whereas this process is not necessary for cold cracks. In the latter case, micro-fractography analysis could be a useful tool or method. Microstructural images [acquired through scanning electron microscopy (SEM)] and diffractograms (X-ray diffraction) are essential for observation, analysis, and prediction of engineering material failures.

This paper describes the microstructure [10] and hardness around the weld joint of 57%Fe15%Cr25%Ni steel plate with 70% reduction and treated by tungsten inert gas (TIG) welding. The instantaneous high heat in welding can generate four regions with different properties and structures. Of these weld areas, HAZ is affected by heat. Welding failure generally stems from the connection among components, especially in HAZ, and can be fatal if neglected. This study aims to understand the characteristics of material around the weld joint to avoid failure when applied. Further works must be conducted to determine welding effects on materials for special purposes, such as structural materials for nuclear power plants.

2. Experimental

The specimen used in the experiment has the following chemical composition (in % wt.): 57.74% Fe, 15.42% Cr, 25.01% Ni, 0.96% Si, 0.34% C, 0.32% Mn, and <0.1% impurities of Ti, S, P, V, Cu, and Nb [4]. After hot rolling with 70% reduction, the steel plate with a dimension of 30 mm × 20 mm × 15 mm was cut into two pieces and subjected to TIG welding with a current of 60 A and a voltage of 50 V (heat input = 1500 J/mm), as shown in Figure 1. Welding was conducted by a qualified welding engineer using special techniques based on Welding Procedure Specification established by professionals in BATAN.
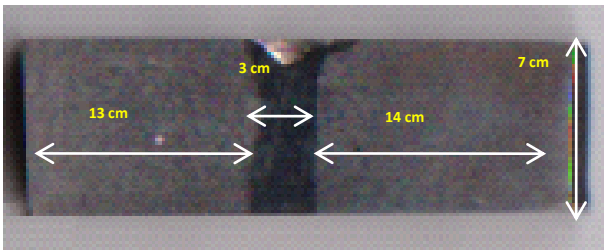
Table 1 shows the welding parameters used in this work. Gas tungsten arc welding (GTAW) was conducted. Prior to welding, the specimen was cleaned with a wind spray

Table 1. TIG Welding Parameters

| Variable	Specification
Weldtype	GTAW
Specimen Dimension	$30 \times 15 \times 7$ cm^3
Gas Protector	Argon
Current	60 A
Voltage	50 V
Speed	120 mm/min

Figure 1. TIG (*tungsten inert gas*) Welding

Figure 2. TIG Welding Macrostructure of the Polished Specimen After Cutting and Etching with A solution Containing 25 ml of HCl, 25 mL of H₂O, and 2.5 ml of HNO₃

to make the specimen tip free from dust impurities when welded. The weld specimen was prepared on the flat side without hem formation and at an angle (butt). In melting, the ends of the metal were glued in the scope of argon gas. Although this method is not a nuclear standard in BATAN, it was carried out to explore different welding methods and improve them in the future. Figure 2 shows the results of the weld test specimen used in this study.

The specimen was gradually ground to remove visible rough surfaces, polished with grid paper (180–2500 mesh) to obtain mirror-like shiny surface, and cleaned with silicone pasta. The surface of the test specimen was etched using a mixture of 25 ml of HCl, 25 ml of H₂O, and 2.5 ml of HNO₃ prior to grain boundary observation on an optical microscope and electron microscope (SEM). Etching was performed by dipping the material surface in etching solution for 30 seconds until the translucent glass became bleak (dop). The specimen was then washed and dried with a dryer. The hardness of the material was diamond indented and determined using Microhardness Vickers Testing Machine in BATAN.

3. Results and Discussion

Microstructure. Figure 3A and B shows the representative microstructures around the weld region. Figure 3A shows the microstructure captured by OM at 400× magnification. In the fusion zone, filler "metal-base" appears to have a columnar dendrite structure [11],[12], pores, and elongated shape due to very rapid cooling (quench) of the molten metal; these characteristics are similar to most cast products, which also have numerous air bubbles trapped in the area. Meanwhile, the metal matrix (BM) has large and small circular net-like microstructure covered by thick and thin grain boundaries. An interesting phenomenon noted in the cast structure is the presence of double-grain boundaries. In the dendrite structure, large structures that form secondary grains follow the pattern of the metal structure of the matrix (the parent). Figure 3B clearly shows the SEM image at 250× magnification.
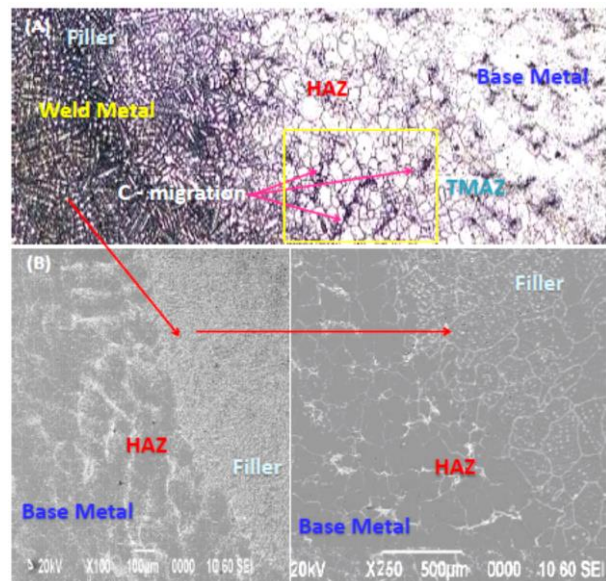
Figure 3. Microstructures of Specimen Around the TIG Weld Joint: (A) Optical Microscope (OM) with 400× Magnification and (B) Electron Microscope with 100× and 400× Magnifications

The interesting phenomenon is visible in the center of the weld. Two phases [8] overlap in the form of cast structure (columnar dendrites) mixed with austenitic structure. The center of the weld metal is dominated by the cast structure. Austenitic grains are also clearly formed in the background probably due to the very rapid decrease in temperature (from melting to room temperature). Moreover, the absence of filler in the welding process induces the cast structure to go back to the original form, i.e., its parent structure of austenite phases.

In Figure 3A, according to the EDX measurements from previous studies [8], the light area contains abundant nickel, otherwise the dark area is poor. Carbon diffuses along the grain boundaries (see blue rectangle in Figure 3A) and looks like a black streak. In the welding area, metal fillers are continuously melted, mixed with the matrix, and heated until the melting temperature. In the weld metal, alloy steel was heated into a liquid at temperatures more than 1200 °C and then rapidly cooled to room temperature of about 25 °C. The rearrangement of the atoms forms an irregular crystal lattice. Small crystals generated of dendritic structure formation. When dendrite growth is mutually reconciled with each other, they can form metal grains and grain boundaries. The indoor cooling mechanism may not be uniform, leading to trapping of numerous air bubbles and forming porous dendrites in the filler BM (weldment) area. In HAZ adjacent to the weld metal, the material undergoes slow cooling to obtain a regular crystal lattice through atom rearrangement. This process of crystal growth broadens and forms grains larger than those in the metal matrix (BM). In HAZ closed to the metal matrix (BM), cooling is faster so that atom rearrangement leads to

brief formation of crystal lattice that can form grains smaller than those in HAZ adjacent to the weld metal (Figure 3A and B). This finding is consistent with the results of mechanical tests, that is, the hardness of the weld metal is approximately 121 HV, which is lower than that of the matrix (BM, about 130 HV). In HAZ adjacent to the weld metal, the hardness is about 116 HV. Grain size is the possible main factor that affects the rise–fall of the hardness value of the material. Small grain size means that more of the grain boundary and high hardness of the material. Therefore, the grain boundary functions as a barrier to the movement of dislocations in the materials. The highest hardness value of 152 HV was found between the base area and the HAZ metal matrix allegedly under the influence of thermo-mechanic process known as TMAZ [14],[15]. The area is very narrow and exposed to the dark lines, which are the path of diffusion of carbon in the grain boun-daries, resulting in hindered movement of dislocations and increased hardness of steel.

Furthermore, some elements, including O from the outer surface (intercept with air) migrate along the grain boundaries to form new colony of precipitates, which coincide and germ in the boundary lines (see yellow rectangle in Figure 4). Colonies form precipitates, such as chromium carbide, aluminum carbide, aluminum oxide, silicone oxide, and silicon carbide [13]. Numerous colonies are found at the outer surface of the material due to their light densities. The colonies move along grain boundaries toward the outer surface and were detected using neutron diffraction technique [13].
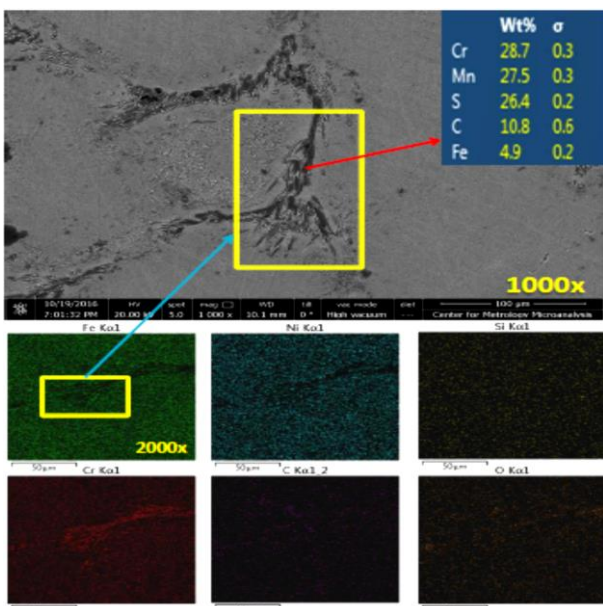

Figure 4. Element Mapping of Fe, Ni, Si, Cr, C, and O (2000×) on the Specimen Surface Around Grain Boundary Containing Precipitates (1000×) Determined by SEM FEI Quanta 650 Equipped with EDX Oxford

The populations (quantity) of Fe, Ni, Si, Cr, C, and O were scanned by EDX spectrometry and displayed by EDS mapping (Figure 4). These precipitates also increase the hardness of the material due to precipitation hardening that can obstruct the movement of dislocations. The precipitate formations are emphasized in literature [16].

Crystal Structure. Changes in the crystal structure due to heat in welding may affect the strength of materials and can be determined through X-ray diffraction measurements around the weld. Figure 5 shows the diffractograms of BM, HAZ, and weld metal taken from the 57Fe15Cr25Ni welded steel specimen by using Shimadzu XD610 with Cu target (1.540 Å). The diffracto-grams show good profiles. The entire diffraction pattern shows five dominant diffraction peaks; this property is typical for a face centered cubic crystal (*fcc*) system. The peaks that appear at successive diffractograms belong to the (111), (200), (220), (311), and (222) planes. These fields are numerically grouped according to all odd or even number and are diffracted around consecutive 2θ *angles* of 44°, 51°, 75°, 91°, and 96.5°.
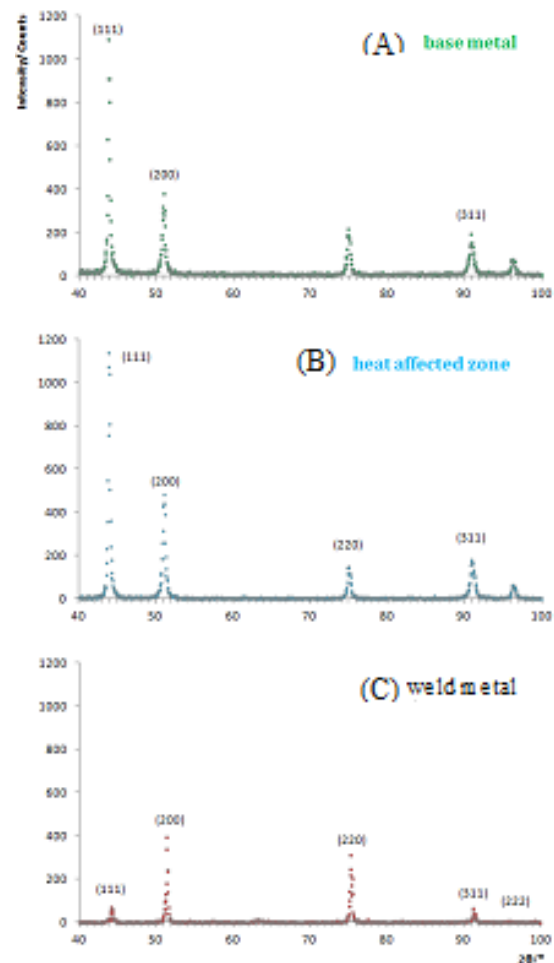

**Figure 5. Crystal Structures of the Specimen Subjected to TIG Welding: (A) BM, (B) HAZ, and (C) Weld Metal**

The diffraction pattern in Figure 4C has lower intensity than the two patterns in Figure 4A and B. Moreover, the (222) plane vanishes in the background. Texturing occurs in the weld metal area. The crystallite orientation changes from (111) plane to (200) and (220) planes.

The weld metal profile broadens (amorphous) and shows full width at half maximum (fwhm) value higher than those in the HAZ and BM areas (Table 2). The weld metal has dendrite structures, and HAZ has grain structures. Thus, surface morphology may affect X-ray scattering. Dendrite structures scatter X-ray broader than grain structures in the diffraction patterns. This finding conforms to the microstructure observations explained above.

Hardness. This parameter can be used to trace the toughness of a material. A material can be fragile and tough because of its hardness. The curve in Figure 6 shows fluctuations in material hardness measured with Microhardness Tester using 200 grf and long load suppression for 15 seconds. The curve is equipped with a line slope to observe the symmetry of heat propagation during welding. The average hardness value of the weld metal along 3 mm (weldmetal) is about 121 HV, which is slightly lower than that of the BM (130 HV). An interesting phenomenon noted in HAZ adjacent to the weld metal is the low hardness value of about 116 HV only. As shown in Figure 5, on the other side, the grains are larger than those in the HAZ area. This finding may be attributed to the nonsymmetrical heat and/or cooling

Table 2. Profile Parameters of the (111) Plane in the Welding Specimen

Specimen	2θ/°	Intensity/counts	fwhm/°
Base Metal	43.75	1092	0.1676
HAZ	43.90	1139	0.2734
Weldment	44.10	72	0.5990
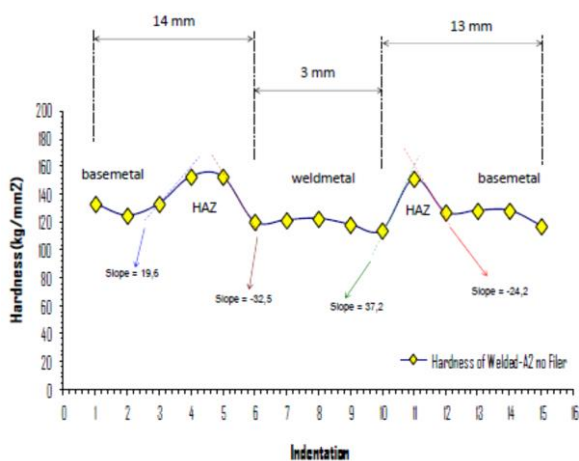
Figure 6. Hardness of TIG Welding Specimen in BM, HAZ, and Weld Metal

of the materials in the welding area; as such, changes in the grain size (microstructure) are more subtle in HAZ adjacent to the BM than those in HAZ adjacent to the weld metal. Thus, the brief hot and cold treatments may influence the hardness of the materials, that is, the hardness value in the regions between the HAZ and weldment is lower than that between HAZ and matrix (BM). The non-symmetric heat propagation is indicated by the higher absolute slope of hardness curves to the right (37.2) than that that of the curve line toward the left (32.5).

Rapid cooling produces brittle materials with high hardness value. This effect is clearly visible in either direction of weldment in HAZ and toward the BM, forming narrow Gaussian curves. BM is not affected by heat and exhibits no changes in the hardness and microstructure. The HAZ region has higher hardness (152 HV) than the weld metal because the former experienced very rapid cooling. Thus, the hardness value increases in very extreme. In terms of microstructure, grains look more uniform and regular than those in the BM. The lowest hardness value was observed in HAZ adjacent to the weld metal (116 HV) due to grain size enlargement as a result of heat generated during welding and slow cooling to room temperature. However, based on hardness data, the average value of hardness in the HAZ is higher than that in the weld metal and BM (about 121 HV). This finding could be due to their black band shown in the microstructure [16],[17] in the area (Figure 6). The migration of carbon is concentrated at the grain boundaries and exhibits a pattern of long dark lines. Other studies [8],[13],[18] reported that chromium carbide ($Cr_{23}C_6$) precipitation could also affect the increase in material hardness.

4. Conclusion

The mechanism of heat welding influenced atom rearrangement and led to the formation of regular and irregular crystal lattice. In rapid cooling, the weld metal was characterized by dendritic, columnar, porous microstructure in the scope of the matrix structure. Meanwhile, the slow cooling effect on the HAZ resulted in more organized crystal lattice with grains larger than those in the metal matrix. The matrix (BM) possessed a circular, net-like microstructure with large and small grains covered by thick and thin boundaries. Texturing occurred in the weld metal area. The crystallite orientation changed from the (111) plane to (200) and (220) planes. The weld metal profile broadened (amorphous), showing fwhm value higher than those in the HAZ and BM areas. This finding conforms to the microstructure observations. The average value of hardness in the weld metal region is about 121 HV, which is slightly lower than that in the BM area (130 HV). In the HAZ region, the average hardness value is

high (about 152 HV). Hence, welding heat can affect the formation of microstructures and the mechanical properties (hardness) of the materials in the weld metal area and the HAZ, which can become brittle and are very critical in responding to the load used.

Acknowledgement

References

[1] N. Effendi, A.K. Jahja, B. Bandriana, W.A. Adi, Urania, Sci. J. Nuc. Fuel Cycle. 18-1 (2012) 48.
[2] R. Rajkolhe, J.G. Khan, Shegaon, Int. J. Res. Adv. Tech. 2-3 (2014) 375.
[3] Parikin, A Technical Reports of DIPA 2016: Presentation, Pranaya Hotel, BSD Serpong, Tangerang Selatan, Banten, 2016, unpublished.
[4] T.H. Priyanto, N. Effendi, Parikin, Adv. Mat. Res. 1123 (2015) 104.
[5] Parikin, N. Effendi, H. Mugihardjo, A.H. Ismoyo, Urania, Sci. J. Nuc. Fuel Cycle. 20-1 (2014) 33.
[6] O.O. Joseph, R.O. Leramo, O.S. Ojudun, J. Mat. Env. Sci. 6-1 (2015) 101.
[7] S.I. Talabi, O.B. Owolabi, J.A. Adebisi, T. Yahaya, Adv. Prod. Eng. Man. 9-4 (2014) 181.
[8] Parikin, A.H. Ismoyo, R. Iskandar, A. Dimyati, Makara J. Tech. 21/2 (2017) 49.
[9] Parikin, T.H. Priyanto, A.H. Ismoyo and M. Dani, Ind. J. Mat. Sci. 17/1 (2015) 22.
[10] M.N.E. Efzan, S. Kesahvanveraragu, J. Emerson, J. Adv. Res. Mat. Sci. 2/1 (2014) 1.
[11] F. Li, Q. Dong, J. Zhang, Y. Dai, Y. Fu, H. Xie, F. Yin, B. Sun, Tran. Non-ferrous Met. Soc. China. 24 (2014) 2112.
[12] F. Li, J. Zhang, F. Bian,Y. Fu, Y. Xue, F. Yin, Y. Xie, Y. Xu, B. Sun, Mat. (Basel). 8-6 (2015) 3701.
[13] Parikin, M. Dani, A.K. Jahja, R. Iskandar, J. Mayer, Int. J. Tech. 8-6 (2017) 1.
[14] T.F.A. Santos, E.A.T. López, E.B. da Fonseca, A.J. Ramirez, Mat. Res. 19-1 (2016) 117.
[15] R. Ramesh, I. Dinaharan, R. Kumar, E.T. Akinlabi, Mat. Sci. Eng. A 687 (2017) 39.
[16] S.R. Nathan, V. Balasubramanian, S. Malarvizhi, A.G. Rao, Def. Tech. 11 (2015) 308.
[17] M. Hajian, A. Abdollah-Zadeh, S.S. Rezaei-Nejad, H. Assadi, S.M.M. Hadavi, K. Chung, M. Shokouhimehr, Mat. & Design 67 (2015) 82
[18] M. Dani, Parikin, A. Dimyati, A.K. Riva'i, R. Iskandar, Int. J. Tech. 8-6 (2017) 10.